# Numerical Study of Nanosecond Pulsed Discharge Effects on Flame Speed and Emissions in Ammonia Flames

Raphael J. Dijoud* and Carmen Guerra-Garcia †
*Massachusetts Institute of Technology, Cambridge, MA, 02139*

**Plasma-assisted combustion of ammonia leverages non-equilibrium electrical discharges to modify flame dynamics and emissions. In this work, we perform a numerical investigation using a one-dimensional model to examine the influence of nanosecond-repetitively pulsed discharges on the propagation of stoichiometric ammonia-air flames at atmospheric conditions. The model incorporates detailed plasma chemistry solved with ZDPlasKin. In particular, we look into the influence of pulse repetition frequency on laminar flame speed and NOx emissions. The simulations reveal unexpected behavior in the spatial distribution of plasma energy deposition within the flame. The plasma is found to significantly speed up the flame, up to +140%, although some numerical challenges prevented us from exploring operation at higher frequencies. The chemical kinetics used also predict a small decrease in $NO$ in the product region of the flame.**

## I. Introduction

Plasma-Assisted Combustion (PAC) refers to the use of plasma to improve or extend the performance envelope of combustion systems [1]. Typically, the plasma is created in the vicinity of a burning or ignitable gaseous mixture through the application of a high electric field between two electrodes. This high voltage will partially ionize the gas, and the produced electrons will be accelerated to form a non-equilibrium plasma, i.e., a plasma where the temperature of the free electrons greatly exceeds that of the heavy species. Those electrons will collide with heavy particles and induce new chemical reaction pathways that modify the local chemistry and can greatly affect the combustion process.

If the voltage is applied for long enough, the heavy species will eventually thermalize and lead to what is often referred to as a "thermal plasma", i.e., a plasma where both the electrons and heavy species have a shared high temperature. This transition to thermal plasma is often considered undesirable, because this phase corresponds to great amounts of energy deposition by the plasma, with limited benefit on the combustion process since most of the energy is deposited thermally. For that reason, research in the field has mostly focused on nanosecond pulsed plasmas, where the electric field is cut-off before reaching the thermalization regime, in most cases. To keep actuating on the combustion process in steady-state, the pulsed discharge is repetitively applied at kilohertz frequencies.

So-called Nanosecond Repetitively Pulsed Discharges (NRPD) have been extensively studied both experimentally and numerically in lab-scale setups, and have been proven to reduce Ignition Delay Time (IDT) [2, 3], lower Minimum Ignition Energy (MIE) [4], extend lean blowout limits [5, 6], curb $NO_x$ emissions [6], and cancel pressure oscillations [7]. Multiple studies have shown benefits using plasma powers below 1% of the flame power. Traditionally, PAC was studied for simple hydrocarbon fuels such as methane or propane. Recently, efforts have focused on characterizing the benefits of plasma assistance for alternative "green" fuels such as ammonia or hydrogen.

In particular, ammonia ($NH_3$) has been the subject of great interest by the community, as PAC is envisioned to potentially address many of the challenges faced by ammonia combustion. Indeed, compared with traditional hydrocarbon fuels, ammonia has a higher auto-ignition temperature, a larger MIE, and a lower Laminar Burning Velocity (LBV). As mentioned above, PAC could potentially help resolve those issues. As a consequence, many research groups have been investigating $NH_3$ PAC, mainly through experimental studies [6, 8–11], but computational works tailored for ammonia PAC have also emerged [12–15]. As a result of this nascent interest, the term PAAC: Plasma-Assisted Ammonia Combustion, has been coined.

Although the impact of plasma assistance on ammonia flames has already been somewhat characterized through studies on IDT, extension of lean blowout limits, and $NO_x$ emissions, comprehensive numerical studies of the effect on the Laminar Burning Velocity (LBV) are scarce. Shahsavari et al. [16] used coupled 0D and 1D codes to model the effect of plasma on the flame speed in an $NH_3/He$/air mixture. The plasma was modeled in 0D, and used as an input

*Ph.D. Candidate, Department of Aeronautics and Astronautics, rdijoud@mit.edu, AIAA Student Member.
†Associate Professor, Department of Aeronautics and Astronautics, guerrac@mit.edu, AIAA Senior Member.

condition for the 1D code. Our approach attempts to dive into more details regarding the coupling between NRPD, flame front, pressure waves, and other transport effects.

The Laminar Burning Velocity (LBV) is a critical combustion metric because it is directly used in large-scale turbulent combustion modeling, along with the heat release rate, and extinction strain rate. Typically, a turbulent combustion code will call external "flamelet libraries" to access what is the local flame consumption rate along the wrinkled flame front based on the local conditions [17]. Therefore, studying the effect of plasma on the LBV is paramount because we can infer the impact on burner-scale performance, while still capturing in detail the physics of the discharge.

## II. One-Dimensional Plasma-Assisted Flame Propagation Model

### A. Model Architecture

The one-dimensional model for plasma-assisted propagation used in this work was presented in earlier papers from our group [18–20]. It is composed of three distinct models: (i) the fluid solver, coded in-house in Julia, (ii) the combustion chemistry solver, which relies on Cantera [21], and (iii) the plasma chemistry solver, based on ZDPlasKin [22] and the Boltzmann solver BOLSIG [23]. Considering the differences in timescales between these different aspects of the problem, we assemble the three models using an operator-splitting scheme method [24].

### B. Governing Equations

The fluid solver models an inviscid adiabatic flow, following the governing equations:

$$\frac{\partial \rho}{\partial t} + \frac{\partial (\rho u)}{\partial x} = 0 \,, \tag{1}$$

$$\frac{\partial (\rho u)}{\partial t} + \frac{\partial (\rho u^2)}{\partial x} = -\frac{\partial p}{\partial x} \,, \tag{2}$$

$$\frac{\partial (\rho e)}{\partial t} + \frac{\partial (\rho u e)}{\partial x} + \frac{\partial}{\partial x}\left(-\lambda \frac{\partial T}{\partial x} + \sum_k j_k h_k\right) = -p \frac{\partial u}{\partial x} \,, \tag{3}$$

$$\frac{\partial (\rho Y_k)}{\partial t} + \frac{\partial (\rho u Y_k)}{\partial x} + \frac{\partial j_k}{\partial x} = 0 \,. \tag{4}$$

The diffusion flux $j_k$ for species $k$ is calculated using a mixture-averaged diffusion approach:

$$j_k^* = -\rho \frac{W_k}{\bar{W}} \bar{D}_k \frac{\partial X_k}{\partial r} \text{ and } j_k = j_k^* - Y_k \sum_m j_m^* \,, \tag{5}$$

where $W$ is the molecular weight and $\bar{D}_k$ is the mixture-averaged diffusion coefficient for species $k$. The domain is initialized at $t = 0$ with a steady-state solution obtained from Cantera [21] for an adiabatic flame.

### C. Boundary Conditions

The one-dimensional domain has two boundaries: the left boundary (fresh gas inflow) and the right boundary (burnt gas outflow). Each boundary has its own boundary condition.

For the left boundary, we used a wave absorption condition, as described by Pavan et al. [19]. This boundary condition allows the pressure wave generated by the plasma to be absorbed at the boundary and avoid unwanted reflections. Concretely, this condition is enforced through the equation

$$\frac{\partial s}{\partial t} = -c \frac{\partial s}{\partial x} \,, \tag{6}$$

where $c$ is the sound speed, and $s = \begin{pmatrix} \rho & u & e \end{pmatrix}$. For the species equations (see equation 4), we enforce a fixed value for the product $\rho Y_k$ at the boundary, corresponding to a mixture close to stoichiometric ammonia-air ($N_2 : O_2 : NH_3 = 617 : 164 : 219$ in moles), at atmospheric conditions ($p = 1\ atm$ and $T = 300\ K$). Initially, the fresh gas flows in through the left boundary at a speed of $1\ cm \cdot s^{-1}$, which corresponds to 10% of the laminar flame speed at those conditions ($S_L = 10\ cm \cdot s^{-1}$).

For the right boundary, the wave-absorption condition was not very effective, and we instead opted to implement an Absorption Sponge Zone (ASZ) [25], similar to what has been used in other one-dimensional models in our group [26, 27]. For each of the governing equations for mass continuity (equation 1), momentum conservation (equation 2), and energy conservation (equation 3), we added an additional term within the ASZ to "force" the convergence towards a desired state. If $\chi$ represents the vectored variable $\chi = \begin{pmatrix} \rho, & \rho u, & \rho e \end{pmatrix}$, then we modify the original equation $f(\chi, t, r)$ into the form

$$\frac{\partial \chi}{\partial t} = f(\chi, t, r) - \sigma \left(x - x_0\right)^2 \left(\chi - \chi_0\right) \ , \tag{7}$$

where $x_0$ refers to the location at which the sponge layer starts, and $\chi_0$ is the desired converged state.

### D. Automatic Mesh Refinement

Our model describes a free flame propagating across the domain [19]. Since the capture of the large gradients close to the flame front calls for a fine mesh at that location, we needed a mesh adaptation algorithm so that it can automatically refine close to the flame front, and coarsen the mesh size when gradients are small. To quantify the mesh error criteria, we used the methodology developed by Löhner [28]. The error at the grid cell $i$ is directly computed from the value of the state variable $s_i$ at that cell and the neighboring cells as

$$E_i = \frac{|\alpha_i s_{i+1} - 2\gamma_i s_i + \beta_i s_{i-1}|}{\alpha_i |(s_{i+1} - s_i)| + \beta_i |(s_i - s_{i-1})| + \epsilon(\alpha_i |s_{i+1}| + 2\gamma_i |s_i| + \beta_i |s_{i-1}|)} \ , \tag{8}$$

where $\alpha_i$, $\beta_i$, and $\gamma_i$ are grid coefficients defined as

$$\alpha_i = \frac{2}{(h_{i+1} + h_i)h_i} \ , \beta_i = \frac{2}{(h_i + h_{i-1})h_i} \text{ and } \gamma_i = \frac{\alpha_i + \beta_i}{2} \ , \tag{9}$$

where $h_i$ is the size of cell $i$. The error metric $E_i$ is non-dimensional and bounded between 0 and 1. The cell $i$ is then refined if the error $E_i$ is above a given threshold, or pruned if the error $E_i$ is below a given threshold.

### E. Plasma Modelling

The plasma is modelled through the plasma kinetic mechanism developed in 2023 at Princeton University for ammonia/air mixtures by Zhong et al. [29]. We also used the combustion chemical kinetics selected by the same group, and later reduced for two-dimensional simulations of plasma-assisted ignition of ammonia, by Shi et al. [30].

A major input for the plasma model is the reduced electric field profile, $E/N$, which, in the cases studied, takes the form:

$$\frac{E}{N}(t, x) = \alpha(x) \times f(t) \ , \tag{10}$$

Where $f(t)$ is a nanosecond-pulse that was measured experimentally and reported by Nagaraja et al. [31]. The pulse is about 10 $ns$ long, and we rescaled it so that the peak $E/N$ is 220 $Td$. The spatial coefficient $\alpha(x)$ introduced in equation 10 represents how the plasma is spatially distributed. In this work, we used different profiles, given in figure 1. We also implemented a maximum threshold energy density deposited by the plasma. Within a specific mesh cell, if the energy deposited by the plasma reaches 0.5 $mJ \cdot cm^{-3}$, then the reduced electric field for the rest of that pulse is set to 0 in that cell.

## III. Dynamics of Plasma Energy Deposition Across the Flame Front

As a preliminary study, we investigated the spatial structure of the energy deposition across the 1D domain, in the case of a uniform reduced electric field between $x = -1.5$ and $x = 0.5$ $cm$ (square profile, see black curve 1 in figure 1). The threshold energy per pulse used for this section was 5 $mJ \cdot cm^{-3}$. We compared the results from the 1D solver with the results given by our 0D solver, when the initial conditions are locally identical to the 1D case. In practice, the only difference between the 0D and 1D results is that the 0D model does not capture transport effects, including convection, heat diffusion, and species diffusion. Keeping the same plasma kinetic mechanism by Zhong [29], we also compared the predictions when the combustion mechanism was not the one developed by Shi et al [30], but the one recently developed at MIT by Doner et al. [32]. Results are shown in figure 2.

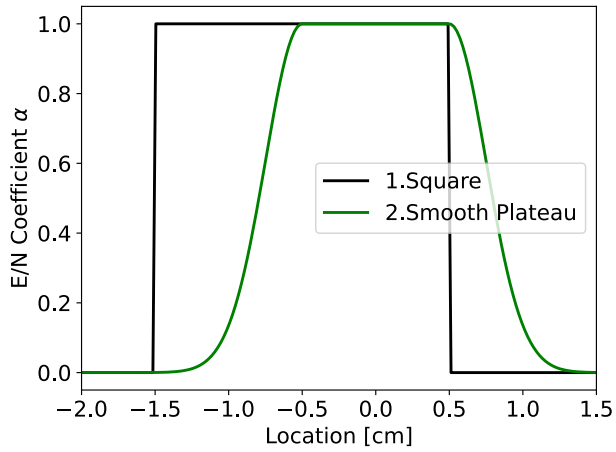


**Fig. 1 Different possible configurations describing the spatial actuation of the plasma within the 1D domain. Initially, the flame is located at $x = 0$.**

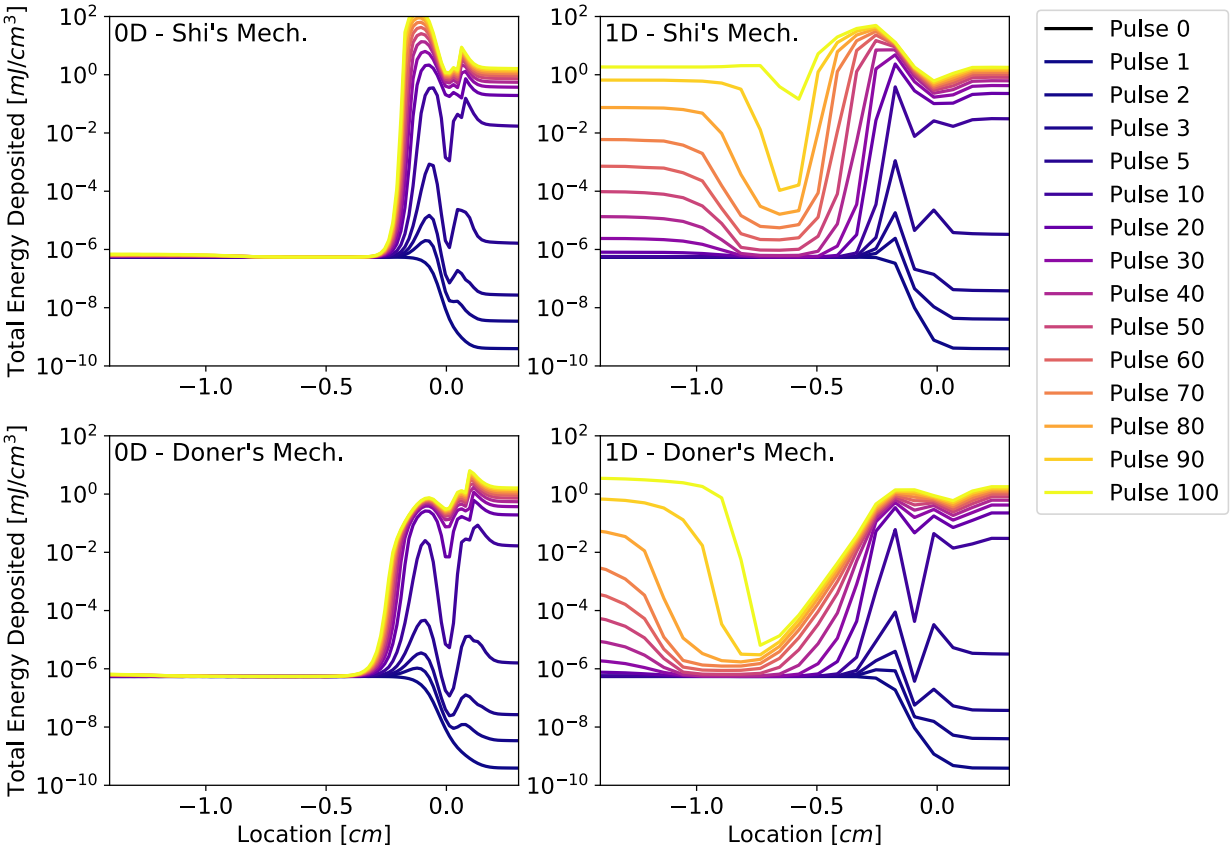


**Fig. 2 Cumulative energy deposited by the plasma from pulses 1 to 100, using combustion mechanism by Shi et al. [30] (top) or Doner et al. [32] (bottom), including transport effects (right) or not (left). Pulse repetition frequency is** $10\ kHz$**.**

First, results shown in figure 2 reveal that there is a significant difference in plasma energy deposition within the reactants between the 0D and 1D configurations, regardless of the combustion mechanism used. In the zero-dimensional case (left plots of figure 2), the energy deposited by the plasma within the reactants remains very low, and most of the

energy is deposited during the initial pulse. In contrast, the one-dimensional case (right plots of figure 2) shows that the energy deposited by the plasma keeps increasing, especially at the edge of the plasma-actuated domain. Regions away from the plasma edge also observe this behavior, although somewhat delayed.

This behavior was unexpected, as it has not been reported for this plasma mechanism, or for others in the literature. Most numerical studies using this chemistry set for combustion have centered on 0D simulations [15, 33–36], which can not capture such spatial dynamics. Taneja et al. [37] modeled streamers in 3D using this mechanism, but only at nanosecond-timescales. Shi et al. [30] did model ignition of ammonia using a simplified version of this plasma mechanism in a 2D simulation, but did not present spatial maps of energy deposition or plasma species. As a result, this unusual behavior may simply have gone unnoticed in prior studies, or it may occur only within the specific physical conditions examined here.

## IV. Effect of Plasma Actuation on Combustion Metrics

### A. Effect on $NO_x$ Emissions

For a given simulation of plasma-assisted propagation of ammonia-air flames, we investigated the effect of the plasma on $NO_x$ and $N_2O$ across the flame. Results are shown in figure 3. We can see that both $NO_2$ and $N_2O$ concentrations in the reactants are significantly increased by the plasma. Concentrations of $NO$ and $N_2O$ at the location of the flame also increase with the plasma. But the domain of interest for $NO_x$ emissions is the product region, and we see no large effect of the plasma in that region, except a mild reduction in $NO$. Indeed, we observed a $NO$ reduction $< 300\ ppm$ across the cases. It is important to note that $NO_x$ chemistry within an ammonia flame is challenging to accurately capture numerically, and this chemical mechanism has not been validated for combustion, only partial oxidation. These pollutant levels are not well captured by current chemical kinetic models for ammonia combustion, and even less so for plasma-assisted ammonia combustion.

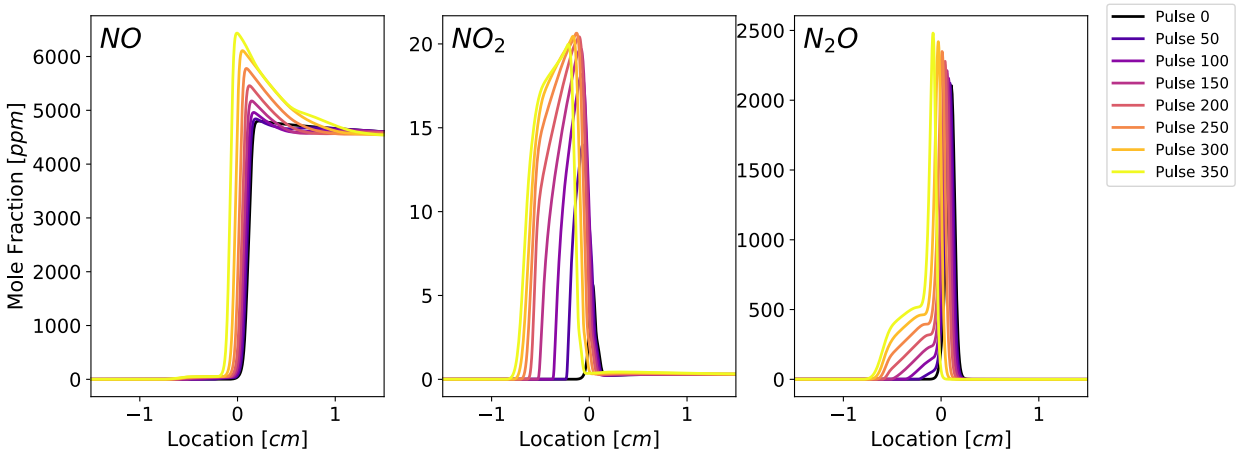


**Fig. 3 Spatio-temporal evolution of the mole fractions of $NO$ (left), $NO_2$ (middle), and $N_2O$ (right), across the flame front, between pulses 0 and 350. The pulse repetition frequency is 25 $kHz$. The plasma is actuated between $x = -1.0$ and $x = 1.0\ cm$ (results obtained using the smooth plateau profile, see green curve 2 in figure 1).**

### B. Effect on Laminar Burning Velocity

Figure 4a shows the evolution of the burning velocity as the flame propagates within the plasma region, for different actuation frequencies. All cases used a "smooth plateau" profile that delimits the plasma region (see green curve 2 in figure 1). We can see that, at high frequencies, the flame decelerates at first when the plasma is activated, before accelerating faster than the baseline laminar flame speed at those conditions, $S_L$. The initial slowdown is caused by the pressure waves generated during the nanosecond pulses ahead of the flame front (which remains the region of highest energy deposition, see top-right of figure 2), which are greatly accentuated as pulse repetition frequency is increased. Eventually, the flame reaches fresh gas that has been pre-activated and pre-heated by the plasma, leading to a progressive

acceleration of the flame and eventually overcoming the effect of the pressure waves. This acceleration of the flame front was observed for all actuation frequencies. We then expect the laminar flame speed to peak or reach a plateau, although we were unable to reach these conditions for the higher frequencies because of numerical issues. Similar behavior has been observed both numerically and experimentally for methane-air flames [20, 38].

Figure 4b summarizes the expected benefit of plasma actuation on laminar flame speed. We compare the present results with earlier work on methane flames by Pavan [19]. Preliminary results for ammonia flames indicate a larger enhancement than previously reported for methane. However, these trends are highly sensitive to both the energy deposition profile and the chemical kinetic model, and therefore can hardly be compared between mixtures. For ammonia, we observe a maximum increase in laminar flame speed of about +140% for $PRF = 25\ kHz$. Values at frequencies larger than $3\ kHz$ have not converged (remaining below the peak) and therefore are reported only for reference. For methane, the dependence of the flame speed enhancement on plasma repetition frequency appears to follow $\frac{\Delta LBV}{S_L} = a \times PRF^n$, where we found that $n = 2$. Further work is needed to better characterize the expected benefit on flame propagation across plasma parameters. Additional work is needed to more thoroughly characterize this scaling and to map the expected benefits across plasma operating conditions. We also note that there may exist an upper limit in PRF at which kinetic and thermal enhancement no longer outweigh early-stage pressure disturbances, though this requires further confirmation.

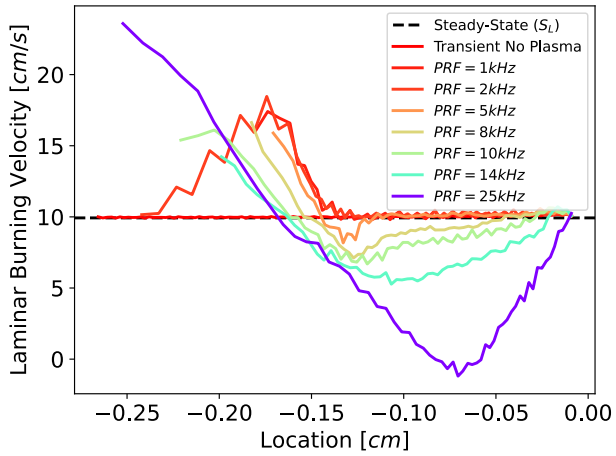


(a) Spatial evolution of the LBV for various PRF.

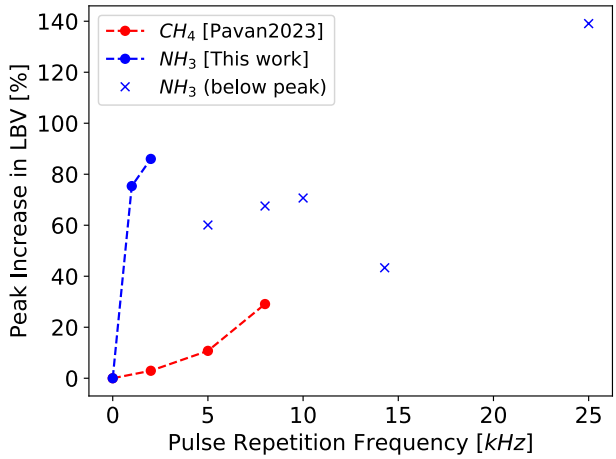


(b) Maximum LBV enhancement as a function of PRF.

**Fig. 4 Effect of plasma actuation on the Laminar Burning Velocity (LBV) as a function of plasma Pulse Repetition Frequency (PRF).**

## V. Conclusion

This work investigates the effect of nanosecond-repetitively pulsed discharges on the propagation of a laminar stoichiometric ammonia-air flame at atmospheric conditions. The numerical solver used combines the ZDPlasKin solver with Cantera and an in-house one-dimensional inviscid adiabatic fluid solver. The preliminary analysis revealed significant differences in plasma energy deposition across the flame depending on whether transport effects are included, suggesting that 1D effects have a large effect on how much energy is deposited by the plasma into the reactants. Simulation results on the combustion metrics show that laminar flame speed is significantly increased, by up to +140% for a pulse repetition frequency of 25 $kHz$. We faced numerical convergence problems that prevented us from reaching steady-state for these high frequency cases. We also found a slight decrease in $NO$ within the products region when plasma was activated up to 6%. The authors call for further work from the community to improve the current plasma and combustion mechanisms, to reliably predict plasma energy deposition, and improve the accuracy of $NO_x$ predictions.

## Acknowledgments

This research was funded by the National Science Foundation (NSF), under Award Number 2339518, and by ExxonMobil.

## References

[1] Ju, Y., and Sun, W., "Plasma assisted combustion: Dynamics and chemistry," *Progress in Energy and Combustion Science*, Vol. 48, 2015, pp. 21–83. https://doi.org/10.1016/j.pecs.2014.12.002.

[2] Bozhenkov, S. A., Starikovskaia, S. M., and Starikovskii, A. Y., "Nanosecond gas discharge ignition of H2- and CH4- containing mixtures," *Combustion and Flame*, Vol. 133, No. 1-2, 2003, pp. 133–146. https://doi.org/10.1016/S0010-2180(02)00564-3.

[3] Kosarev, I. N., Aleksandrov, N. L., Kindysheva, S. V., Starikovskaia, S. M., and Starikovskii, A. Y., "Kinetics of ignition of saturated hydrocarbons by nonequilibrium plasma: CH4-containing mixtures," *Combustion and Flame*, Vol. 154, No. 3, 2008, pp. 569–586. https://doi.org/10.1016/j.combustflame.2008.03.007.

[4] Tropina, A. A., Uddi, M., and Ju, Y., "On the effect of nonequilibrium plasma on the minimum ignition energy: Part 2," *IEEE Transactions on Plasma Science*, Vol. 39, No. 12 PART 1, 2011, pp. 3283–3287. https://doi.org/10.1109/TPS.2011.2160570.

[5] Pilla, G. L., Lacoste, D. A., Veynante, D., and Laux, C. O., "Stabilization of a swirled propane-air flame using a nanosecond repetitively pulsed plasma," *IEEE Transactions on Plasma Science*, Vol. 36, No. 4 PART 1, 2008, pp. 940–941. https://doi.org/10.1109/TPS.2008.927343.

[6] Choe, J., Sun, W., Ombrello, T., and Carter, C., "Plasma assisted ammonia combustion: Simultaneous NOx reduction and flame enhancement," *Combustion and Flame*, Vol. 228, 2021, pp. 430–432. https://doi.org/10.1016/j.combustflame.2021.02.016.

[7] Shanbhogue, S. J., Dijoud, R. J., Pavan, C. A., Rao, S., Campo, F. G. D., Guerra-Garcia, C., and Ghoniem, A. F., "Emissions and Dynamic Stability Improvements in Premixed CH4/NH3 Swirling Flames with Nanosecond Pulsed Discharges," *AIAA Aviation Forum and ASCEND, 2024*, 2024. https://doi.org/10.2514/6.2024-3898.

[8] Sun, J., Bao, Y., Ravelid, J., and Ehn, A., "Emission Spectroscopy of Nanosecond Pulsed Plasma Discharges in Ammonia/Air Flames," *25th International Symposium on Plasma Chemistry*, 2023.

[9] Aravind, B., Yu, L., and Lacoste, D., "Enhancement of lean blowout limits of swirl stabilized NH3-CH4-Air flames using nanosecond repetitively pulsed discharges at elevated pressures," *Applications in Energy and Combustion Science*, Vol. 16, 2023, p. 100225. https://doi.org/10.1016/J.JAECS.2023.100225.

[10] Wang, Y., Kong, C., Ao, J., Li, H., Wang, C., Wu, X., and Zhang, Z., "A phenomenological understanding of the multimodal low-frequency oscillating combustion of ammonia induced by filamentary plasma discharge," *Combustion and Flame*, Vol. 270, 2024, p. 113748. https://doi.org/10.1016/J.COMBUSTFLAME.2024.113748.

[11] Kim, G. T., Park, J., Chung, S. H., and Yoo, C. S., "Effects of non-thermal plasma on turbulent premixed flames of ammonia/air in a swirl combustor," *Fuel*, Vol. 323, 2022, p. 124227. https://doi.org/10.1016/J.FUEL.2022.124227.

[12] Shioyoke, A., Hayashi, J., Murai, R., Nakatsuka, N., and Akamatsu, F., "Numerical Investigation on Effects of Nonequilibrium Plasma on Laminar Burning Velocity of Ammonia Flame," *Energy and Fuels*, Vol. 32, No. 3, 2018, pp. 3824–3832. https://doi.org/10.1021/acs.energyfuels.7b02733.

[13] Taneja, T. S., Johnson, P. N., and Yang, S., "Nanosecond pulsed plasma assisted combustion of ammonia-air mixtures: Effects on ignition delays and NOx emission," *Combustion and Flame*, Vol. 245, No. 112327, 2022, p. 112327. https://doi.org/10.1016/j.combustflame.2022.112327.

[14] Faingold, G., and Lefkowitz, J. K., "A numerical investigation of NH3/O2/He ignition limits in a non-thermal plasma," *Proceedings of the Combustion Institute*, Vol. 38, No. 4, 2021, pp. 5849–5857. https://doi.org/10.1016/j.proci.2020.08.033.

[15] Mao, X., Zhong, H., Liu, N., Wang, Z., and Ju, Y., "Ignition enhancement and NOx formation of NH3/air mixtures by non-equilibrium plasma discharge," *Combustion and Flame*, Vol. 259, 2024, p. 113140. https://doi.org/10.1016/J.COMBUSTFLAME.2023.113140.

[16] Shahsavari, M., Konnov, A. A., Valera-Medina, A., and Jangi, M., "On nanosecond plasma-assisted ammonia combustion: Effects of pulse and mixture properties," *Combustion and Flame*, Vol. 245, 2022, p. 112368. https://doi.org/10.1016/J.COMBUSTFLAME.2022.112368.

[17] Poinsot, T., and Veynante, D., *Theoretical and Numerical Combustion*, 2nd ed., Edwards, 2001.

[18] Pavan, C. A., and Guerra-Garcia, C., "Modelling the Impact of a Repetitively Pulsed Nanosecond DBD Plasma on a Mesoscale Flame," *AIAA Science and Technology Forum and Exposition, AIAA SciTech Forum 2022*, 2022, pp. 1–13. https://doi.org/10.2514/6.2022-0975.

[19] Pavan, C., "Nanosecond Pulsed Plasmas in Dynamic Combustion Environments," Ph.D. thesis, Massachusetts Institute of Technology, Cambridge, USA, 2023. URL https://dspace.mit.edu/handle/1721.1/151492.

[20] Pavan, C. A., and Guerra-Garcia, C., "Laminar flame speed modification by Nanosecond Repetitively Pulsed Discharges, Part I: Numerical model," *Combustion and Flame*, Vol. 282, 2025, p. 114484. https://doi.org/10.1016/J.COMBUSTFLAME.2025.114484.

[21] Goodwin, D. G., Moffat, H. K., Schoegl, I., Speth, R. L., and Weber, B. W., "Cantera: An object-oriented software toolkit for chemical kinetics, thermodynamics, and transport processes (version 2.6.0)," *https://www.cantera.org*, 2022. https://doi.org/10.5281/zenodo.6387882, URL https://www.cantera.org.

[22] Pancheshnyi, S., Eismann, B., Hagelaar, G. J., and Pitchford, L. C., "Computer code ZDPlasKin," *http://www.zdplaskin.laplace.univ-tlse.fr*, 2008. URL http://www.zdplaskin.laplace.univ-tlse.fr.

[23] Hagelaar, G. J., and Pitchford, L. C., "Solving the Boltzmann equation to obtain electron transport coefficients and rate coefficients for fluid models," *Plasma Sources Science and Technology*, Vol. 14, No. 4, 2005, pp. 722–733. https://doi.org/10.1088/0963-0252/14/4/011.

[24] McNamara, S., and Strang, G., "Operator Splitting," *Splitting Methods in Communication, Imaging, Science, and Engineering*, edited by R. Glowinski, S. J. Osher, and W. Yin, Springer, 2016. URL http://www.springer.com/series/718.

[25] Zhou, Y., and Wang, Z. J., "Absorbing boundary conditions for the Euler and Navier-Stokes equations with the spectral difference method," *Journal of Computational Physics*, Vol. 229, No. 23, 2010, pp. 8733–8749. https://doi.org/10.1016/j.jcp.2010.08.007.

[26] Dijoud, R. J., Pavan, C. A., and Guerra-Garcia, C., "Numerical Model of the Initiation and Propagation of a Radial Flame by Nanosecond Pulsed Discharges," *AIAA SciTech Forum and Exposition, 2023*, 2023. https://doi.org/10.2514/6.2023-0747.

[27] Dijoud, R. J., "Ignition by Nanosecond Repetitively Pulsed Discharges," *Massachusetts Institute of Technology SM Thesis*, 2023. URL https://dspace.mit.edu/handle/1721.1/154175.

[28] Löhner, R., "An adaptive finite element scheme for transient problems in CFD," *Computer Methods in Applied Mechanics and Engineering*, Vol. 61, No. 3, 1987, pp. 323–338. https://doi.org/10.1016/0045-7825(87)90098-3.

[29] Zhong, H., Mao, X., Liu, N., Wang, Z., Ombrello, T., and Ju, Y., "Understanding non-equilibrium N2O/NOx chemistry in plasma-assisted low-temperature NH3 oxidation," *Combustion and Flame*, Vol. 256, 2023, p. 112948. https://doi.org/10.1016/J.COMBUSTFLAME.2023.112948.

[30] Shi, Z., Mao, X., Wang, Z., and Ju, Y., "Numerical Study of NH3 /H2/Air Ignition in Nanosecond Plasma Discharges with Non-Equilibrium Energy Transfer," *AIAA SciTech Forum 2025*, 2025. https://doi.org/10.2514/6.2025-2311.

[31] Nagaraja, S., Yang, V., Yin, Z., and Adamovich, I., "Ignition of hydrogen-air mixtures using pulsed nanosecond dielectric barrier plasma discharges in plane-to-plane geometry," *Combustion and Flame*, Vol. 161, No. 4, 2014, pp. 1026–1037. https://doi.org/10.1016/j.combustflame.2013.10.007.

[32] Doner, A. C., Cao, C., Pekkanen, T. T., Shirish Zalte, A., Grinberg Dana, A., and Green, W. H., "Detailed Kinetic Model for Combustion of NH3/H2 Blends," *14th U.S. National Combustion Meeting*, 2025.

[33] Zheng, Z., Hu, Y., Cao, R., Rong, W., Zhao, F., and Yu, W., "Kinetic roles of energy transformation during ignition enhancement of NH3/air mixture by non-equilibrium plasma discharge via nanosecond repetitive pulsed discharge," *Combustion and Flame*, Vol. 275, 2025, p. 114061. https://doi.org/10.1016/J.COMBUSTFLAME.2025.114061.

[34] Wang, Z., Aravind, B., Mashruk, S., and Valera-Medina, A., "Numerical investigation on the combustion characteristics of premixed NH 3-air flames using gliding arc plasma," 2025. https://doi.org/10.1016/j.joei.2025.102314.

[35] Gillingham, H., Lesaffre, T., and Barléon, N., "A semi-analytical model for Plasma-Assisted Combustion: Application to NH3-H2-air mixtures," *Combustion and Flame*, Vol. 283, 2026, p. 114528. https://doi.org/10.1016/J.COMBUSTFLAME.2025.114528.

[36] Dijoud, R. J., and Guerra-Garcia, C., "Energy Pathways in Plasma-Assisted Ignition of Ammonia," *AIAA Science and Technology Forum and Exposition, AIAA SciTech Forum 2025*, 2025. https://doi.org/10.2514/6.2025-0165.

[37] Sanjeev Taneja, T., Sitaraman, H., and Yang, S., "1D modeling of plasma streamers at ammonia-air flame conditions," *Journal of Physics D: Applied Physics*, Vol. 58, 2025, p. 16. https://doi.org/10.1088/1361-6463/ad7ecb.

[38] Pavan, C. A., and Guerra-Garcia, C., "Laminar flame speed modification by nanosecond repetitively pulsed discharges, Part II: Experiments," *Combustion and Flame*, Vol. 282, 2025, p. 114475. https://doi.org/10.1016/J.COMBUSTFLAME.2025.114475.